Heliyon 10 (2024) e27773

Contents lists available at ScienceDirect

Heliyon

journal homepage: www.cell.com/heliyon

Research article

Design, synthesis and in silico molecular docking evaluation of novel 1,2,3-triazole derivatives as potent antimicrobial agents

Sudhakar Reddy Baddam [a,**], Mahesh Kumar Avula [b,c], Raghunadh Akula [b], Venkateswara Rao Battula [d], Sudhakar Kalagara [e], Ravinder Buchikonda [b], Srinivas Ganta [f], Srinivasadesikan Venkatesan [g], Tejeswara Rao Allaka [h,*]

[a] University of Massachusetts Chan Medical School, RNA Therapeutic Institute, Worcester, MA, 01655, United States
[b] Technology Development Center, Custom Pharmaceutical Services, Dr. Reddy's Laboratories Pvt. Ltd., Hyderabad, Telangana, 500049, India
[c] Department of Organic Chemistry and FDW, Andhra University, Visakhapatnam, Andhra Pradesh, 530003, India
[d] Department of Chemistry, AU College of Engineering (A), Andhra University, Visakhapatnam, Andhra Pradesh, 530003, India
[e] Department of Chemistry and Biochemistry, University of the Texas at El Paso, El Paso, TX, 79968, United States
[f] ScieGen Pharmaceutical Inc., Hauppauge, NY, 11788, United States
[g] Department of Chemistry, School of Applied Science and Humanities, VIGNAN's Foundation for Science, Technology and Research, Vadlamudi, Andhra Pradesh, 522213, India
[h] Centre for Chemical Sciences and Technology, Institute of Science and Technology, Jawaharlal Nehru Technological University Hyderabad, Kukatpally, Hyderabad, Telangana, 500085, India

ARTICLE INFO

Keywords:
Benzooxepines
Chalcones
1,2,3-Triazoles
Biological evaluations
Docking interactions
ADMETlab2.0

ABSTRACT

Chalcone and triazole scaffolds have demonstrated a crucial role in the advancement of science and technology. Due to their significance, research has proceeded on the design and development of novel benzooxepine connected to 1,2,3-triazolyl chalcone structures. The new chalcone derivatives produced by benzooxepine triazole methyl ketone **2** and different aromatic carbonyl compounds **3** are discussed in this paper. All prepared compounds have well-established structures to a variety of spectral approaches, including mass analysis, ^{1}H NMR, ^{13}C NMR, and IR. Among the tested compounds, hybrids **4c**, **4d**, **4i**, and **4k** exhibited exceptional antibacterial susceptibilities with MIC range of 3.59–10.30 μM against the tested *S. aureus* strain. Compounds **4c**, **4d** displayed superior antifungal activity against *F. oxysporum* with MIC 3.25, 4.89 μM, when compared to fluconazole (MIC = 3.83 μM) respectively. On the other hand, analogues **4d**, **4f**, and **4k** demonstrated equivalent antitubercular action against H_{37}Rv strain with MIC range of 2.16–4.90 μM. The capacity of ligand **4f** to form a stable compound on the active site of CYP51 from *M. tuberculosis* (1EA1) was confirmed by docking studies using amino acids Leu321(A), Pro77(A), Phe83(A), Lys74(A), Tyr76(A), Ala73(A), Arg96(A), Thr80(A), Met79(A), His259(A), and Gln72(A). Additionally, the chalcone–1,2,3–triazole hybrids ADME (absorption, distribution, metabolism, and excretion), characteristics of molecules, estimations of toxicity, and bioactivity parameters were assessed.

* Corresponding author.
** Corresponding author.
E-mail addresses: sudhakar.baddam@umassmed.edu (S.R. Baddam), tejajntuh18@gmail.com (T.R. Allaka).

https://doi.org/10.1016/j.heliyon.2024.e27773
Received 11 September 2023; Received in revised form 6 March 2024; Accepted 6 March 2024
Available online 24 March 2024

1. Introduction

The 13th leading cause of death worldwide is tuberculosis. Approximately 10 million new cases and 1.5 million deaths have been reported globally in 2020, with 2,14,000 of the deaths being related to HIV. TB [1]. The lack of treatment for multidrug–resistant *tuberculosis* (MDR–TB) and extremely drug–resistant *tuberculosis* (XDR-TB) in 2020 will ensure the ongoing need for the development of new anti–TB medications with unique mechanisms [2,3]. The present goal is to develop an effective anti-TB agent that has a short course of therapy, is less complicated, toxic, drug-resistant, and has few drug-drug interactions [4]. Since 1950, laboratory and clinical research have used the highly virulent *Mycobacterium* TB $H_{37}Rv$ strain [5]. Out of the twenty human cytochrome P450 (CYP51) enzymes expressed by Mtb $H_{37}Rv$ genome, CYP121A1 has been demonstrated to be crucial for mycobacterial growth or survival in the host [6]. Therefore, CYP51 is regarded as a key targets for the development of anti–TB drugs. The scientific community, which is working to create new and effective therapies for human diseases, is faced with a tremendous difficulty due to the high level of resistance that bacteria have acquired to antimicrobial drugs already available on the market [7]. Therefore, it is imperative to create therapeutic agents with increased potency for treating of broad–spectrum microbial infections, such as those brought on by methicillin–resistant *S. aureus* (MRSA), methicillin–resistant *S. epidermidis* (MRSE), and vancomycin–resistant *S. aureus* (VRSA) as well as extended spectrum β–lactamases (ESBL) [8].

One of the most researched scaffolds is chalcone, which is present in many naturally occurring compounds and has been extensively used in the advancement of science and technology. It has been employed as dynamic intermediates in the synthesis of several heterocyclic compound with added value [9,10]. It also plays a crucial part in many biological activities as a result of its special structure with Michael acceptor features, which makes them tolerant to various biomolecules and causes them to react or interact with them [11–13]. On the other hand, chalcones are the building blocks for flavonoids and isoflavonoids and exhibit diverse biological properties. These properties may be explained by the suppression of various molecular targets, such as antibacterial [14], antifungal [15], antitubercular [16], anti–inflammatory, analgesic [17], antioxidants [18], anti–plasmodia [19], anticancer activity [20], anti–consultant activity [21], and anti-hyperglycemic molecules [22]. However, benzooxepines have a significant role in medicinal chemistry, hormones, nucleic acids and therapeutic medicines [23]. They also constitute a central motif in heterocyclic chemistry. These compounds are well–known pharmacophores with potent anti–disease effects, including anti–TB, anti–HIV, anti–fungal, antibacterial, and anticancer activity in the central nervous system [24–31].

Nitrogenous heterocyclic molecules had a significant role in the discovery of novel organic and medicinal compounds. Due to its advantages of flexible structure, high selectivity, high efficiency, and low toxicity, as well as their compatibility with the development idea of modern green chemistry, triazole scaffolds have attracted interest in the pharmaceutical industry [32]. Finding antimicrobial drugs that are both more efficient and less harmful is therefore a major research priority. In this context, novel pharmacological agents for medicinal chemistry can be found in both the quinoline and triazole compounds, both are based on nitrogen containing hetercyclics [33]. 1,2,3–Triazoles are found in varying bioactive compounds and shown numerous biological potentials like antimicrobial [34], anticancer [35], anti–allergic [36], anti–inflammatory [37], immunosuppressant [38], antiviral, anti–HIV [39], antimalarial [40], anticonvulsant [41], antidiabetic [42], analgesic, and anti–oxidant activities [43]. As seen in Fig. 1, nitrogen-containing heterocyclic

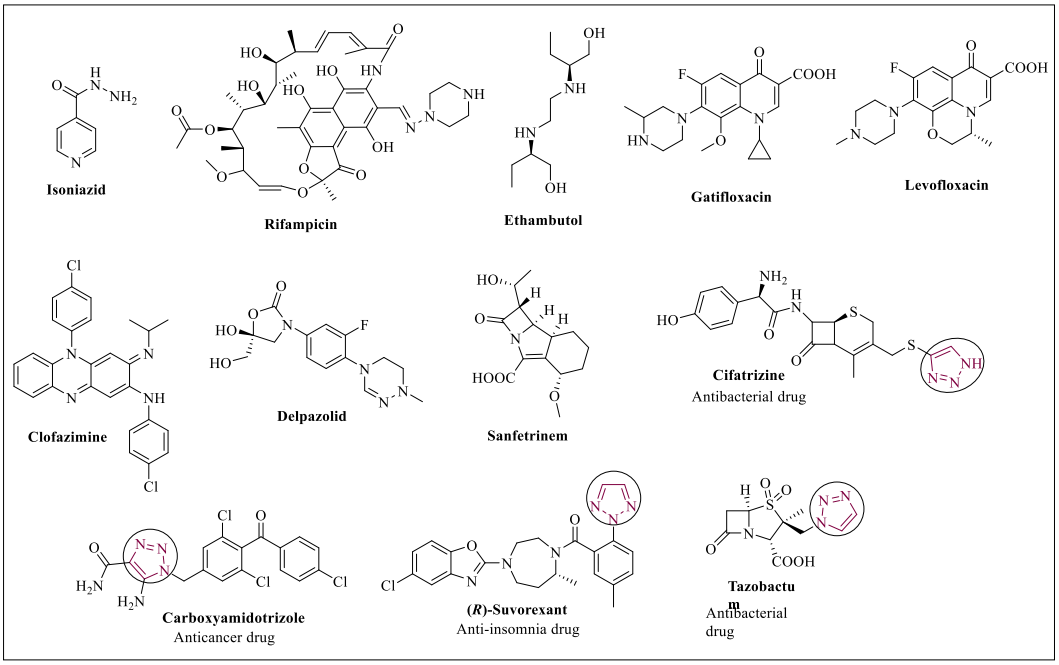

Fig. 1. Commercial chemical structures of the reported anti-TB active molecules and 1,2,3-triazoles.

compounds are well-documented in the literature for the treatment of various diseases including fatal tuberculosis because of their exceptional biological activity patterns.

In order to characterise the behaviour of a small molecules in the binding site of target proteins as well as to shed light on basic biochemical processes, docking techniques have been one of the most fundamental and significant approaches for drug discovery [44]. It allows atomic-level molecular interactions between a bound ligand and a protein to be predicted. Our research intends to bind benzooxapine to 1,2,3-triazole and chalcone systems to enhance inhibitory and biological effects. All of the compounds' predicted drug-likeness was also made public. By combining molecular interactions, biological activity, and molecular level studies, the structure activity connection was optimized. Molecular descriptive analysis, incorporating SwissADME (http://www.swissadme.ch), SwissADMETlab2.0 (https://admetmesh.scbdd.com) online web servers was used to investigate the active sites in compounds [45]. The cytochrome P450 enzymes called sterol 14α-demethylases (CYP51) are essential for the manufacture of sterols in eukaryotes. They are also the primary targets of antifungal drugs and may be used in the future to treat protozoan infections. Human CYP51 was once thought to be a viable target for cholesterol-lowering medications (statins, which are currently being studied for cancer) but it turned out to have a high intrinsic resistance to inhibition [46]. The remarkable success of statins, which are today the most often prescribed drugs, led to the abandonment of several attempts to create CYP51 inhibitors as cholesterol-lowering treatments [47]. In order to understand the molecular basis for the human enzyme's resistance to inhibition, we used site-directed mutagenesis in conjunction with comparative structure/functional analysis of CYP51 orthologs from various biological kingdoms. We also designed, synthesised, and characterized new compounds. Using Human CYP51 as the target, we have conducted a thorough molecular modelling study to determine the binding mechanism and important active site interactions (cation–Π, Π–Π, H-bonding, and σ–σ) of the ligands in order to estimate their binding affinity of 1EA1 protein. The solubility of drug candidate molecules in various bodily fluids is determined by the lipophilicity parameter, which is correlated with the molecule's behavior in the biological environment and its ADMET profile.

2. Results and discussions

2.1. Chemistry

The target compounds **4a–k** were synthesised by a two-step procedure as shown in Scheme 1, Fig. 2. Firstly, the azidation of 5-chloro-4-(chloromethyl)-2,3-dihydrobenzo [*b*]oxepine through nucleophilic aromatic substitution afforded 4-(azidomethyl)-5-chloro-2,3-dihydrobenzo [b] oxepine **1** [48]. Scheme 1 illustrates the synthetic technique for 1,2,3–triazole analogues. Compound 4-(azidomethyl)-5-chloro-2,3-dihydrobenzo [*b*]oxepine **1** was synthesised using 3,4-dihydrobenzo [b]oxepin-5(2H)-one, in accordance with a previously published method and it was used to enolate-mediated triazole synthesis without any additional purification [49]. Triazole methyl ketone **2**, a frequent intermediate, was produced in good yield over two steps with acetylacetone (0.024 mol) in 30 mL of DMF in the presence of TEA (0.048 mol). Using aryl aldehydes **3a–k** (0.0101–0.0130 mol) in EtOH, the common intermediate **2** was subjected to catalytic aldol condensation and then chilled in an ice bath. After 10 min of constant stirring, a sodium hydroxide ethanolic solution (0.152 mol, 6.08 g) was added to the mixture drop-wise. After that, the reaction mixture was brought to room temperature and stirred continuously overnight. It was first diluted with 200 mL of ice-cold water before being neutralized with HCl solution. After filtering, excess ice-cold water was used to wash the produced solid, and it was then dried to produce pure (*E*)-chalcones **4a–k** with a 1,2,3-triazole scaffold. Electron-rich and electron-poor aryl groups were successfully added to the products as an aryl group conjugated with an enone molecule.

Initially, we devoted our effort to establish the optimized reaction conditions and the coupling reaction of 1-(1-((5-chloro-8-methyl-2,3-dihydrobenzo [*b*]oxepin-4-yl)methyl)-5-methyl-1H-1,2,3-triazol-4-yl)ethan-1-one (**2**) with benzaldehyde (**3a**) in EtOH was used as a model reaction for this purpose. The study was initiated by carrying out the reaction at 40 °C for 4 h under basic $NaHCO_3$ condition in DMF to obtained 55% yields (Table 1, entry 1). The desired product **3a** was obtained in not acceptable yield when the reaction

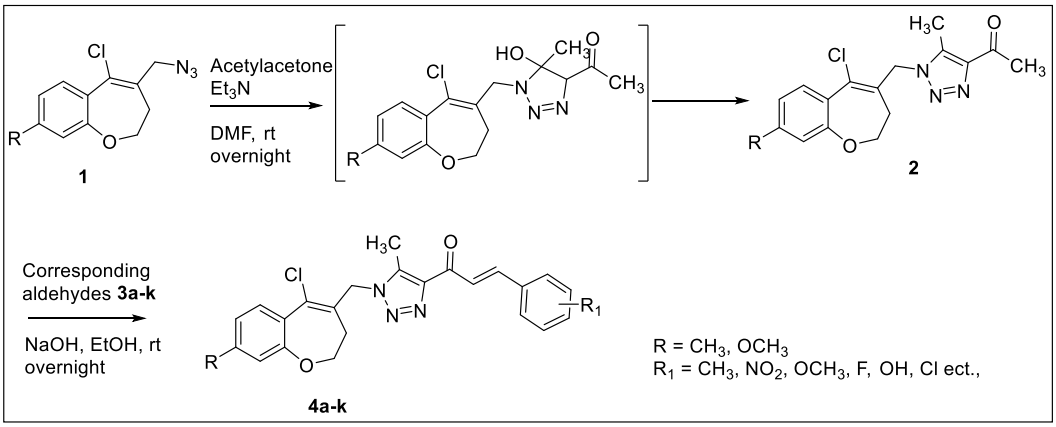

Scheme 1. Design strategy of benzooxepine−1,2,3−triazoles linked to chalcones.

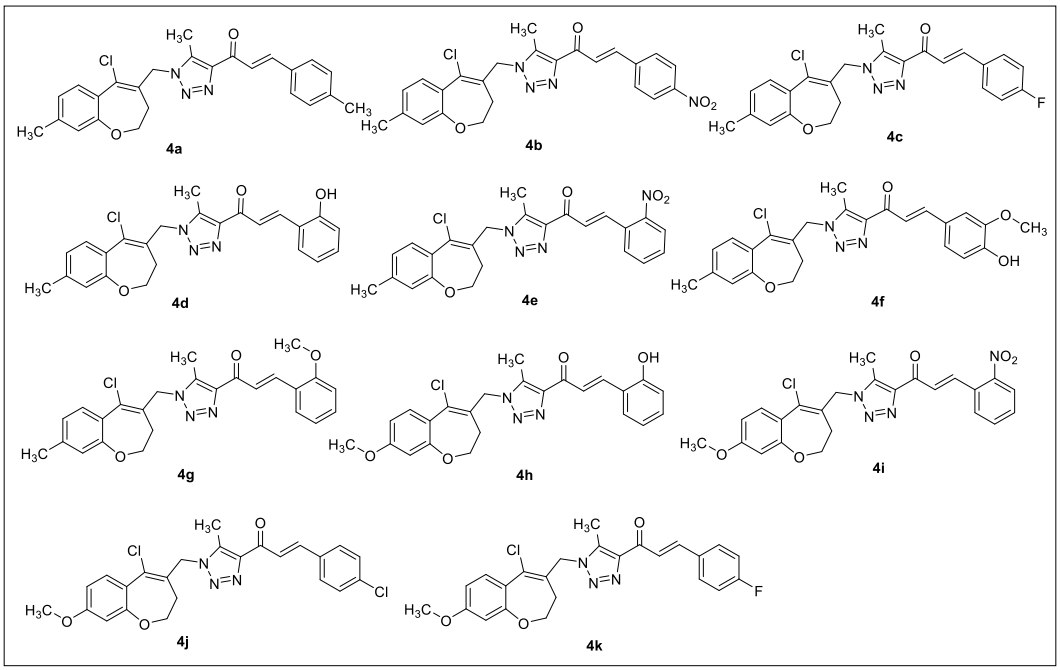

Fig. 2. List of 1,2,3–triazole benzooxepine chalcone derivatives.

Table 1
Optimization conditions on the coupling of **2** with **3a**.[a].

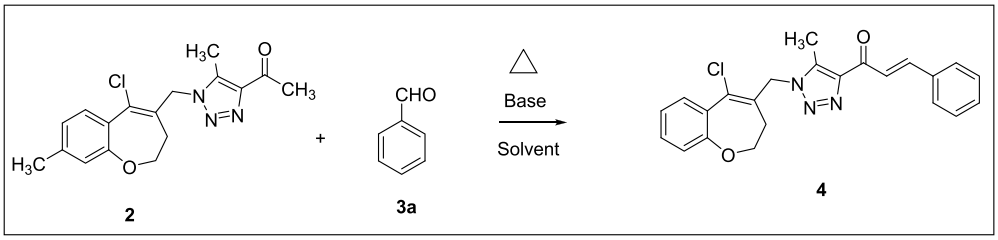

S.No.	Base	Solvent	Temp. (°C)	Time	Yields (%)
1	$NaHCO_3$	DMF	40 °C	4 h	55
2	$NaHCO_3$	Acetone	50 °C	4 h	36
3	$NaHCO_3$	MeOH	rt	6 h	60
4	$NaHCO_3$	EtOH	rt	6 h	62
5	NaOH	DMF	40 °C	4 h	65
6	NaOH	Acetone	40 °C	4 h	59
7	NaOH	MeOH	rt	10 h	67
8	NaOH	EtOH	40 °C	12 h	70[b]
9	NaOH	EtOH	rt	24 h	88[c]

[a] All reactions were performed using the **2** (0.0042 mol), **3a** (0.0051 mol), NaOH (0.076 mol) and in EtOH (12 mL) under inert atmosphere.
[b] The reaction was performed in the absence of rt.
[c] Isolated yields.

temperature was increased to 50 °C in acetone (entry 3, Table 1). While the reaction time was incresead for obtained good yields (60%) was observed under MeOH, $NaHCO_3$ basic conditions (entry 3, Table 1). Indeed, the reaction was com pleted within 6 h in ethanol and employing the basic $NaHCO_3$ at room temperature to give few more yields (62%) (entry 4, Table 1). Moreover, it was noted that further increse the % of yields and decrese in the reaction time to 4 h did not affect the product yields (entry 5, Table 1). Coupling product was isolated in 59% yield (entry 6, Table 1) by the reaction between 2 and 3a in the presence of NaOH in acetone as aprotic solvent at 40 °C was sluggish. Our coupling reaction of ketone **2** and benzaldehyde **3a** with 10 vol of methanol at rt for 10 h resulted in 67% yield of 1,2,3-triazole derivative **4a** after silica gel chromatography (entry 7, Table 1). By conducting the reaction under refluxing conditions

where the product yield was dramatically reduced even after allowing the reaction to proceed for a longer length, the role of conventional reaction was evaluated (entry 8, Table 1). Motivated by these outcomes, we then concentrated on the potential for increasing the product yield even more. As a result, the reaction was conducted with 10 vol of ethanol, NaOH (0.076 mol), and ketone (**2**, 0.0042 mol) in isolation. Since entering condition 9 produced the best results for the manufacture of 4a, that was investigated for the preparation of the necessary 1,2,3-analogues.

The structures of the synthesised compounds were elucidated by the ^{1}H NMR, ^{13}C NMR, IR and mass spectral analysis. The structure of the titled compound **4a** was deduced from IR spectrum, which showed the absorption bands of the –CH and =CH functional groups at 2926.21 cm^{-1}, 3205.20 cm^{-1}. Moreover, a vibrational frequency at 1660.81 cm^{-1} corresponding to the –CO moiety and two singlet signals of C]C and COC at ν 1541.24 and 1218.53 cm^{-1} respectively. The ^{1}H NMR spectra of compound **4a** showed the appearance of a singlet signal at δ 4.48 ppm pointing to the –CH_2 protons of the adjacent triazole moiety and two triplet signals at δ 4.36, 2.97 ppm corresponding to the benzooxepine –CH_2 protons respectively. Furthermore, this compound disclosed the appearance of two signals of two –CH_3 protons of the phenyl, benzooxepine moieties at δ 3.61, 2.16 ppm and two doublet signals at δ 8.30 and 6.92 ppm referring to ethylene group. The other two boublet signals at δ 7.91, 7.54 ppm, related to the *p*-tolyl hydrogens, and the boublet signals δ at 7.71, 7.65 ppm, corresponding to the aromatic protons of the benzooxepine ring. The ^{13}C NMR spectra of compound **4a** revealed three signals δ at 69.7, 55.2, and 22.6 ppm, referring to –CH_2, –CH_3 carbons of the benzooxepine moiety. Meanwhile, the two signals at δ 144.2 and 126.8 ppm corresponding to the two methylene carbons and one signal at δ 185.8 ppm relating to the carbonyl carbon. Remaining signals δ at 149.7, 134.6 ppm, related to the triazole carbons, in addition the remaining carbon signals at δ 155.1 to 110.9 ppm corresponding to the aromatic carbons of this moiety. Ultimately, the assigned structures of compounds **4a-k** were validated by mass data. For every molecule *m/z* values, the molecular ion peak $[M + H]^{+}$ were nearly in agreement with the calculations.

2.2. Antibacterial and antifungal activity

The antibacterial efficacy of the substances listed was assessed using three Gram–(+ve) microorganisms [*Bacillus subtilis, Streptococcus pneumoniae*, and *Staphylococcus aureus*], two Gram-negative bacteria [*Escherichia coli* and *Pseudomonas aeruginosa*] and along with two fungus strains *Candida albicans* and *Fusarium oxysporum* [50,51]. The values of MICs for the tested benzooxepine-triazole derivatives are listed in Table 2. Regarding the *S. aureus* bacterial strain, both benzooxepine derivatives linked to 4-fluorophenyl −1,2,3-triazole (**4c**) and 2-hydroxyphenyl-1,2,3-triazole (**4d**) exhibited more effective and equal antibacterial activities with MIC values of 3.82 and 3.59 μM, respectively. Compounds **4i** and **4k** exhibited decreased antibacterial activity against *S. aureus* with MIC values of 8.22 and 10.30 μM, respectively. Compounds **4a**, **4b**, and **4e** showed poor antibacterial activities against *S. aureus* with MIC values of 67.33, 76.14, and 58.02 μM, respectively. Finally, with respect to the tested *B. Subtilis* bacterail strain, triazoles **4c, 4d** and **4i** were discovered to be the most active compounds with MICs of 5.79, 6.13, and 3.01 μM, whereas remaining analogues **4a**, **4f**, **4k** showed moderate to good antibacterial activity against Gram-positive bacteria *B. Subtilis* with their MICs 21.45, 24.77, 10.30 μM respectively. The substances tested against the *B. Subtilis* organism with MIC values (>100 μM), *p*-nitrophenyl benzoxapine chalcone (**4b**), *o*-nitrophenyl benzoxapine chalcone (**4e**), and *p*-chlorophenyl benzoxapine chalcone (**4j**), did not exhibit any antibacterial action. However, the synthesised chalcone 1,2,3-triazle compounds **4d, 4e,** and **4i** demonstrated increased antibacterial activities against *S. pneumoniae* strain with MIC values of 7.11, 8.20, and 15.30 μM, respectively. According to the data recorded in Table 2, Benzooxepine-1,2,3-triazole derivatives **4a**, **4d**, and **4k** were found to be the most potent agents against the *E. coli* bacterial strain, with MIC values of 13.56, 15.92, and 6.20 μM, respectively. Regarding the *E. coli* microorganism, the triazole compounds **4b**, **4e**, and **4h**

Table 2
Results of antimicrobial activity and anti-TB activity of the tested compounds.

S.No.	Antibacterial activity MIC (μM) Gram-positive strains		Gram-negative strains			Antifungal activity		Anti-TB MIC (μM)
	S. aureus	*B. Subtilis*	*S. pneumoniae*	*E. coli*	*P. aeruginosa*	*C. albicans*	*F. oxysporum*	H_{37}Rv
4a	67.33	21.45	>100	13.56	20.47	>100	16.38	>100
4b	76.14	>100	34.76	21.06	13.65	28.45	>100	12.65
4c	3.82	5.79	33.64	>100	14.26	38.10	3.25	42.57
4d	3.59	6.13	7.11	15.92	5.90	>100	4.89	3.12
4e	58.02	>100	8.20	19.03	16.23	54.24	>100	30.60
4f	24.77	14.23	72.10	20.92	>100	76.11	22.55	4.90
4g	>100	55.72	66.72	81.30	43.19	>100	58.02	>100
4h	32.15	42.67	>100	25.91	19.42	65.79	41.79	>100
4i	8.22	3.01	15.30	42.04	4.12	30.61	>100	44.12
4j	40.51	>100	21.73	>100	33.76	25.52	16.31	37.25
4k	10.30	14.29	18.02	6.20	>100	16.24	5.29	2.16
MXF[a]	3.53	3.07	4.21	5.08	4.49	ND	ND	ND
FZL[b]	ND	ND	ND	ND	ND	3.08	3.83	ND
SPM[c]	ND	ND	ND	ND	ND	ND	ND	1.34

ND means biological activity was not detected.
[a] MXF: Moxifloxacin.
[b] FZL: Fluconazole.
[c] SPM: Streptomycin.

exhibited more effective antibacterial activities and contributed MICs 21.06, 19.03, 25.91 μM, whereas *p*-fluorophenyl benzoxapine chalcone (**4c**), *p*-chlorophenyl benzoxapine chalcone (**4j**) did not shown antibacterial activity. It is worth mentioning that compounds **4b**, **4d**, and **4i** showed good antibactericidal properties as it displayed equal MIC values of 13.65, 5.90, and 4.12 μM against Gram-negative microorganism *P. aeruginosa* when comapred to reference MXF [4.49 μM].

Triazole compounds **4c**, **4d**, and **4k** demonstrated excellent antifungal activity against the tested organisms *F. oxysporum*, which is comparable to the activity of the standard drug Fluconazole. In contrast, triazole compounds **4b**, **4j**, and **4k** were potent antifungal activity against fungal strain *C. albicans* with MIC values at 28.45, 25.52, and 16.24 μm, respectively. In comparison to normal medication under the same circumstances, the remaining compounds **4f**, **4h**, and **4j** have moderate antifungal efficacy against both fungal strains (Table 2). F (Compound **4c**) > CH_3 (compound **4a**) and F (Compound **4k**) > Cl (compound **4j**) were thus the sequence in which the 4−substituted phenyl derivatives exhibited inhibitory effects, respectively. Moreover, compound **4d**, the hydroxy derivative, exhibited greater potency compared to compound **4e**, the nitro derivative, among the 2-substituted phenyl derivatives. One interesting finding about the chalcone triazole compounds' inhibitory antibacterial activity is that the size of the aryl groups has a significant impact on the activities that are seen. With the exception of compounds **4d** and **4k**, which had MIC values of 2.16 and 3.12 μM, the anti-TB activity data, which are displayed in Table 2 and Fig. 3, showed that compounds **4a–k** were much more potent than the conventional inhibitor streptomycin [1.34 μM]. The most active compounds were 4-nitrophenyl, and 3-methoxy-4-hydroxyphenyl derivatives with MIC values 12.65 μM, 4.90 μM (compounds **4b**, and **4f**, respectively). Furthermore, compounds **4c**, **4e** and **4i** with 4-fluorophenyl-1,2,3-triazole, 2-nitrophenyl-1,2,3-triazole, and 2-nitrophenyl-1,2,3-triazole substituents, respectively, exhibited moderate to good anti-TB activity (MIC values = 42.57, 30.60, 44.12 μM), whereas remaining triazole-chalcone derivatives **4a**, **4g**, and **4h** are inactive.

2.3. Docking pose interactions

The X-ray crystallographic structure of human Cytochrome P450 14α-sterol demethylase (CYP51) from *Mycobacterium tuberculosis* in complex with fluconazole was obtained from the Protein Databank [1EA1 (www.rcsb.org),] in order to perform a molecular docking study aimed at shedding light on the potential binding modes and the crucial binding features of the synthesised hybrids (**4a–k**) with CYP51 domain of human Cytochrome P450 [52–55]. The fact that the relevant substrates exhibit both strong hydrophobic interactions and a profusion of hydrogen bonds when docked to the Cytochrome P450 compartment is particularly noteworthy, as seen in Figs. 4 and 5 and Table 3. To validate our biological findings, the synthesised benzooxapine−chalcone compounds were docked against the CYP51 protein. According to reports, the residues Tyr76(A), Leu321(A), Gln72(A), Pro77(A), Phe83(A), Lys74(A), Ala73(A), His259 (A), Arg96(A), Thr80(A), and Met79(A) interact with the active site of 5-fluorouracil (5-FU). In comparison to the native streptomycin binding score of −7.89 kcal/mol, compounds **4d**, **4f**, and **4k** generally had a similar binding pattern in the binding site of *Mycobacterium tuberculosis*. These compounds had estimated docking energy scores of −10.0, −9.12, and −10.23 kcal/mol, respectively. The most active ligand **4d** had some hydrophobic (Π−alkyl) interactions is formed with important amino acids such as Met79(A), Val395 (A) X 2, His392(A), Leu321(A), Leu100(A), Arg96(A) X 2. Furthermore, N14 atom of triazole ring of **4d** hybrid formed one hydrogen bond with NH_2 of Arg96(A) [2.93 Å] and in addition other two hydrogen bonding formation between O11 of benzooxepine with NE2 of Gln72(A) [3.08 Å], and O28 of orthophenyl with NH of Ile323(A) [2.75 Å] amino acids respectively (Fig. 4). Similarly, Pi-Pi bond is formed between 1,2,3-triazole ring and phenyl ring of Tyr76(A) with bond distance 2.99 Å, besides one Π−lone pair interaction was formed with Met433(A) [3.21 Å]. However, this ligand formed four carbon hydrogen bonding interactions with Arg96(A), His392(A), Val395(A), Leu321(A) amino acid residues, whereas it had highest Van der Waals stackings with Arg95(A), Arg391(A), Phe255(A), Val434(A), Pro320(A), His259(A), Val435(A), Ile322(A), Leu324(A), Phe78(A) amino acids in the active site of *M. tuberculosis*.

Curiously, the **4f** ligand, which had the highest Cytochrome P450 demethylase inhibitory activity, also had the highest energy binding score, which was −9.12 kcal/mol and inhibition-constant (204.96 nM) higher than that of the reference compound. This hybrid was also demonstrated an effective binding pattern with the important amino acid residues in the target protein. Through the establishment of two hydrogen bonds with bond distances of 2.93 Å and 2.87 Å between O29 of α,β-unsaturated carbonyl carbon and

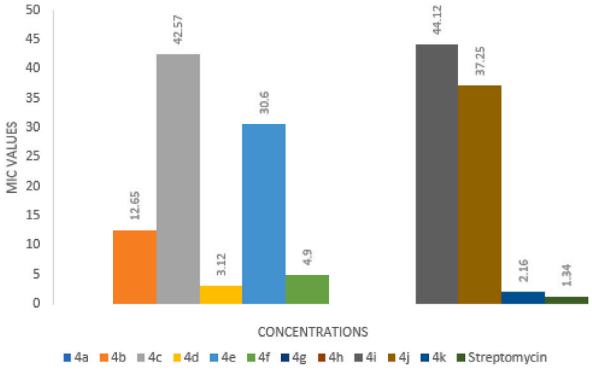

Fig. 3. Antitubercular activity profile of final chalcone bearing 1,2,3−triazole derivatives.

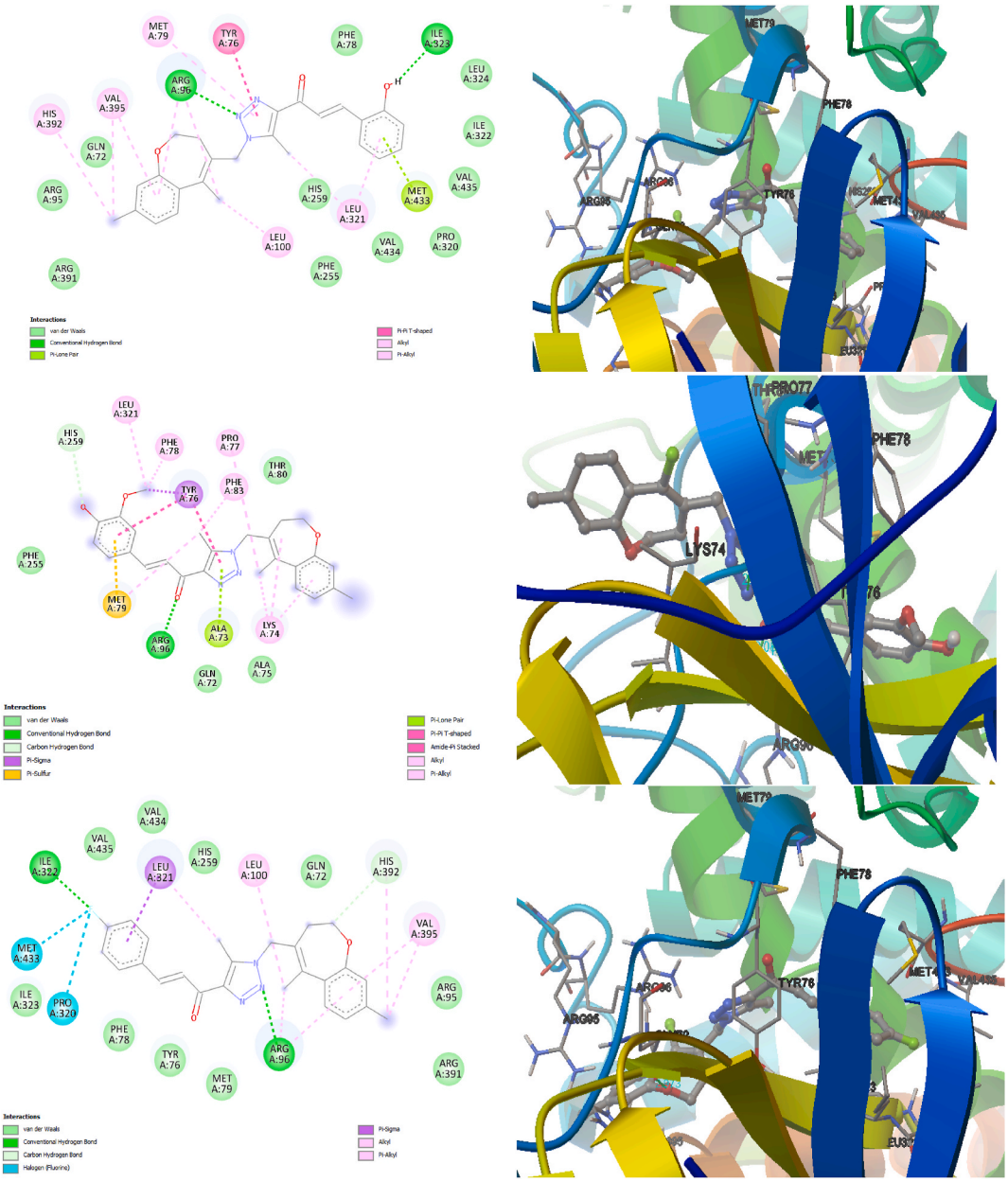

Fig. 4. 2D-, 3D-docking conformations of the most active 1,2,3-triazole ligands (**4d**, **4f**, and **4k**) against CYP51 from *M. tuberculosis* [PDB: 1EA1].

NH1, NH2 of Arg96(A), it was able to connect well with the cytochrome pocket. Additionally, the 1,2,3−triazole, phenyl moiety of **4f** was able to form two Pi-Pi interactions with Tyr76(A) amino acid with bond distances 3.35 Å, 2.83 Å, which considered one of the crucial interactions that underlying the mechanism of CYP51 inhibition. Furthermore, It also formed highest hydrophobic interactions (Π−alkyl) with Leu321(A), Phe78(A), Pro77(A), Phe83(A) X 2, Lys74(A) X 3, Met79(A) (Π−sigma), and Tyr76(A) (Π−sulphur) interactions in the active site of Cytochrome P450 14 alpha-sterol demethylase (CYP51) from *M. tuberculosis.* Meanwhile, this 1,2,3-triazole ligand displayed five van der Waals stackings with Phe255(A), His259(A), Gln72(A), Ala75(A), Thr80(A) amino acid residues. Besides, in the middle of this receptor, the benzooxapine moiety showed four carbon hydrogen interactions with Thr80(A), Ala73(A), Lys74(A), Met79(A) amino acids. The other most active ligand **4k** was found to bind with the Cytochrome P450 pocket via H-bonds with Ile322(A) [F33···N,], Arg96(A) [N14···NH2] amino acids with bond distance 3.11 Å, 3.00 Å respectively. Other interactions (Van der Waals) were stabilized in this binding pocket of the backbone through binding with Ile32(A), Phe78(A), Tyr76(A), Met79(A), Arg391(A), Arg95(A), Gln72(A), His259(A), Val434(A), and Val435(A). Moreover, 4k hybrid together with halogenated binding interactions with Met433(A), Pro320(A) amino acids and exhibited one Π−sigma bonding with Leu321(A) amino acid residue. Moreover, this ligand exhibited promising binding modes as OCH_3−, phenyl group binds via Π−alkyl stackings with Val395(A) amino acid,

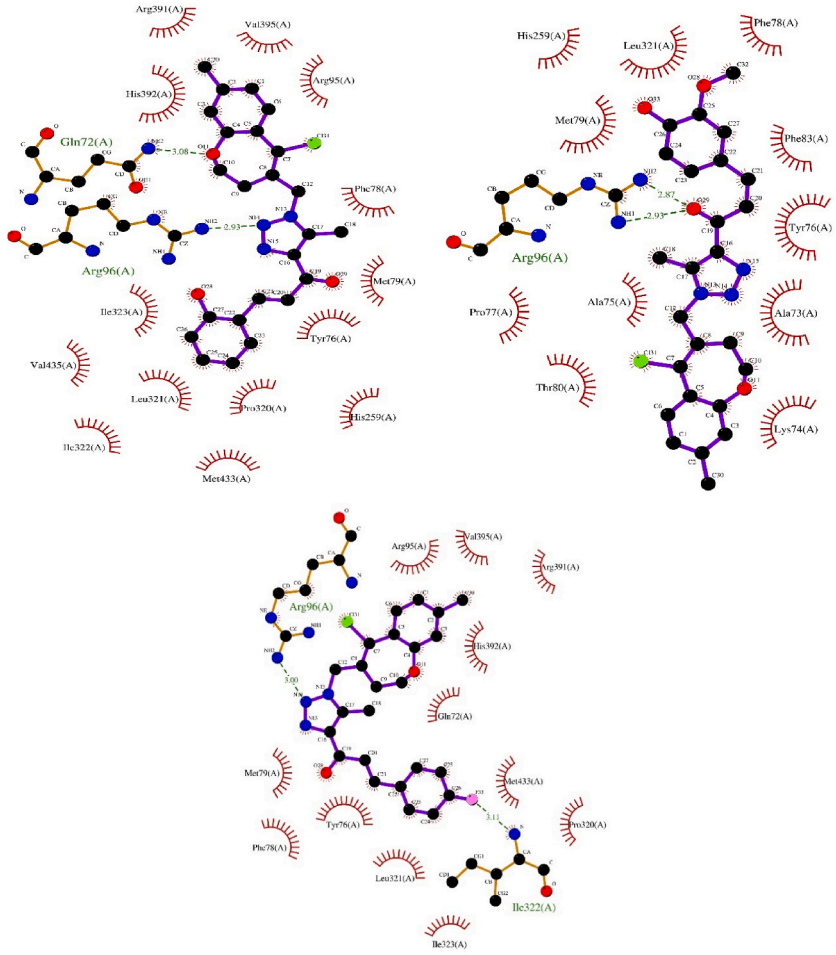

Fig. 5. Ligplot docking poses of most active 1,2,3−triazolylchalcone derivatives (**4d**, **4f**, and **4k**) within the active site of CYP51 from *M. tuberculosis*.

as well as the chlorine atom of the benzooxepine ring, phenyl group participated with two Π−alkyl bonds with Arg96(A) and Leu100 (A) amino acids in the active site Cytochrome P450 pocket of *M. tuberculosis* (Fig. 4). On the other hand, this hybrid showed good fitting with this pocket via formation of three strong carbon hydrogen bondings with Leu321(A), His392(A), and Arg96(A) respectively.

3. *In silico* physicochemical and pharmacokinetics studies

Using the SwissADME website (http://www.swissadme.ch/index.php), the physicochemical characteristics and drug-likeness of chalcones based benzooxepine-1,2,3-triazole **4a–4k** were determined [56]. The Molsoft LLC website, https://www.molsoft.com/mprop/, was utilized to calculate the drug-likeness scores. Novel medications and formulations are chosen based on their physicochemical qualities, which include molecular weight, solubility, molar refractivity, topological polar surface area, and hydrogen bonding capabilities. As a result, these properties of triazoles **4a–k** (Table 4) are crucial for identifying novel drug candidate and should be in accordance with the various rule-based filterates [57]. Based on the findings, we discovered that every produced triazole complies with the five drug similarity guidelines (Lipinski, Ghose, Veber, Egan, and Muegge rules) and is approved as a unique drug candidate [58]. In accordance with this rule, we discovered that the compounds **4c**, **4f**, **4h**, **4j**, and **4k** had the highest ratings for drug-likeness 0.03, 0.02, 0.05, 0.45, and 0.36, respectively and were therefore deemed to be drug like pharmaceuticals (Fig. 6). On the other hand, the two compounds **4e** and **4b** had negative drug-likeness ratings of −0.63 and −0.38 respectively, indicating that they were not-like drugs (Table 4). As a result, Caco-2 cell permeability has been a crucial indicator for the new medication. When a target compounds projected value is > -5.15 log cm s^{-1} (green), it is deemed to fit proper Caco-2 permeability. Based on this rule, we found that the final derivatives **4a–k** have a fit proper Caco-2 permeability within the range of −4.839 to −4.943 log cm s^{-1}.

The toxic properties of benzooxepine-based chalcones **4a–k** was calculated using ADMETlab 2.0 website https://admetmesh.scbdd.com/service/evaluation/cal and all the properties were summed in Table 4 [59,60]. An key component of risk assessment for novel medications is human hepatotoxicity, or H-HT. With a predicted value of 0.3–0.7 (yellow) for moderate toxicity and a strong toxicity value of 0.7–1.0 (red), the new target compounds are either non-toxic for the liver, H-HT negative, with a value of 0–0.3 (green), or

Table 3
Different docking pose interactions in complex with antitubercular drug candidate CYP51with 1EA1 protein.

Ligands	ΔG (Kcal/mol)/ kl (nM)	Bond distance	Amino acid interactions
4d	−10.00/46.45	2.99 Å 3.21 Å 2.93 Å [N14···NH2], 2.75 Å [O28···NH], 3.08 Å [O11 … NE2]	Π−alkyl interactions: Met79(A), Val395(A) X 2, His392(A), Leu321(A), Leu100(A), Arg96(A) X 2 Π−Π stacking: Tyr76(A) Π−lone pair interaction: Met433(A) Hydrogen bondings: Arg96(A), Ile323(A), Gln72(A) Carbon Hydrogen bondings: Arg96(A), His392(A), Val395(A), Leu321(A) Van der Waals: Arg95(A), Arg391(A), Phe255(A), Val434(A), Pro320(A), His259 (A), Val435(A), Ile322(A), Leu324(A), Phe78(A)
4f	−9.12/204.96	3.35 Å, 2.83 Å 2.78 Å 2.93 Å [O29···NH1], 2.87 Å [O29···NH2]	Π−alkyl interactions: Leu321(A), Phe78(A), Pro77(A), Phe83(A) X 2, Lys74(A) X 3 Π−Π stackings: Tyr76(A) X 2 Π−lone pair interaction: Ala73(A) Hydrogen bondings: Arg96(A), Arg96(A) Carbon Hydrogen bondings: Thr80(A), Ala73(A), Lys74(A), Met79(A) Π−sigma: Met79(A), Π−sulphur: Tyr76(A) Van der Waals: Phe255(A), His259(A), Gln72(A), Ala75(A), Thr80(A)
4k	−10.23/37.75	3.11 Å [F33···N], 3.00 Å [N14···NH2]	Π−alkyl interactions: Leu100(A), Val395(A) X 2, His392(A), Arg96(A) X 2, Leu321 (A) Halogenated bonds: Met433(A), Pro320(A) Hydrogen bondings: Ile322(A), Arg96(A) Carbon Hydrogen bondings: Leu321(A), His392(A), Arg96(A) Π−sigma: Leu321(A) Van der Waals: Ile32(A), Phe78(A), Tyr76(A), Met79(A), Arg391(A), Arg95(A), Gln72(A), His259(A), Val434(A), Val435(A)

toxic for the liver, H-HT positive, with two categories. Consequently, chemicals 4d and 4h, which had high predicted values of 0.097 and 0.112, respectively, are categorised as serious carcinogens. At the same time, the other compounds are categorised as moderate to exceptional carcinogens, with predicted ranges of 0.118–0.216.

These days, the metabolism prediction model has focused on how target substances interact with cytochromes P450 mono-oxygenase enzymes (CYP1A2, CYP2C19, CYP2C9, CYP2D6, CYP3A4), which are concentrated in the liver and catalyse the phase 1 metabolism of pharmaceuticals. Table 4 demonstrates that all chalcone based 1,2,3-triazoles **4a–k** were predicted as inhibitors of four enzymes with the probability value ranging from 0.561 to 0.965. To achieve this goal, the Brain Or IntestinaL estimated permeability approach (BOILED-Egg) was introduced as a successful prediction model based on small molecule lipophilicity and polarity calculations [61]. The physicochemical zone of chemicals that are most likely to be absorbed by the GI tract appears to be the white section of the egg, or the yolk. The compounds **4b**, **4c**, **4d**, **4f**, and **4i** that had obvious oral bioavailability were placed on top of the BROILED-Egg, as seen in Fig. 7.

A target compound is considered to have a high passive MDCK permeability when a Papp is more than 20×10^{-6} cm s^{-1} (green). Table 4 illustrates that all the target compounds **4a–k** has a high passive MDCK permeability of more than 20×10^{-6} cm/s in a range from 1.7×10^{-5} to 5.4×10^{-5} cm s^{-1}. Accordingly, all the eleven compounds are inhibitors for P-glycoprotein with values renaging of 0.053–0.883 respectively. On the other hand, triazole based compounds **4g**, **4j**, **4k** are moderate P-glycoprotein inhibitors, but **4a**, **4c** are non-inhibitors of P-glycoprotein. The plasma protein binding (PPB) and percentage unbound in plasma (FU) of the drugs have an impact on how they behave pharmacodynamically. If the expected values of PPB and FU are greater than or equal to 5% (green) and less than 90% (green), respectively, then the target drug is said to have proper plasma protein binding. On the other hand, drugs with a strong plasma protein binding of greater than 90% (poor, red) and a predicted value for FU less than 5% may have a low therapeutic index and less effective cell membrane passage. Based on the information above, it can be concluded that the 1,2,3-triazoles **4a–k** linked to benzooxepine have a high binding with plasma protein, with predicted values of more than 90% (ranging from 96.39% to 99.71%) and less than 5% for FU. Additionally, these compounds may have a low therapeutic index and only marginal membrane-crossing efficiency.

4. DFT studies

All the computations of Density Functional Theory (DFT) was carried out using the Gaussian 16 suite of program. The best inhibitors observed in molecular docking studies were considered for DFT studies. The geometry optimization of the molecules **4d**, **4f**, and **4k** were employed at B3LYP/6-31g (d,p) level of theory in the gas phase. The optimized molecule futher employed using frequency calculation to confirm the optimized molecule have no imaginary frequency. All the molecules have the doublet multiplicity with the charge is zero. The computational method B3LYP was chosen due to the hybrid functional leads several successful results. All the optimized structures of the best inhibitors identified by molecular docking studies were shown in Figs. 8 and 9. The single point energy calculation of the respective molecules were carried out at B3LYP/6-31g (d,p) in the gas phase. The HOMO-LUMO pictures the molecules were depicted in Figure Sx (see Supporting information). The HOMO-LUMO gap a molecule 4D was observed to be low as 1.83 eV. The other two molecules also shown the HOMO-LUMO gap as 1.95 and 1.84 eV for **4f** and **4k**, respectively. The low HOMO-

Table 4
Predicted ADMET properties of synthesised chalocone compounds.

Properties	4a	4b	4c	4d	4e	4f	4g	4h	4i	4j	4k
M.Wt.	433.93	464.90	437.89	435.90	464.90	465.93	449.93	451.93	480.90	470.35	353.89
nRot	5	6	5	5	6	6	6	6	7	6	6
nHBA	4	6	5	5	6	6	5	6	7	5	6
nHBD	0	0	0	1	0	1	0	1	0	0	0
TPSA	57.01	102.83	57.01	77.24	102.83	86.47	66.24	86.47	112.06	66.24	66.24
Mlogp	3.66	2.54	3.83	2.91	2.54	2.59	3.12	2.38	2.03	3.39	3.28
LogD	4.37	4.39	4.25	4.11	4.28	3.92	4.18	3.90	4.09	4.18	4.03
LogS	-6.26	-6.36	-6.09	-5.78	-6.26	-5.61	-6.05	-5.73	-6.21	-6.47	-6.00
Lipinski filter violations	Yes /0	Yes /0	Yes /0	Yes /0	Yes /0	Yes /0	Yes /0	Yes /0	Yes /0	Yes /0	Yes /0
Ghose filter violations	Yes /0	Yes /0	No /1	Yes /0	Yes /0	Yes /0	Yes /0	Yes /0	No /1	Yes /0	Yes /0
Veber filter violations	Yes /0	Yes /0	Yes /0	Yes /0	Yes /0	Yes /0	Yes /0	Yes /0	Yes /0	Yes /0	Yes /0
Egan filter violations	Yes /0	Yes /0	Yes /0	Yes /0	Yes /0	Yes /0	Yes /0	Yes /0	Yes /0	Yes /0	Yes /0
Muegge filter violations	Yes /1	Yes /0	Yes /0	Yes /0	Yes /0	Yes /0	Yes /0	Yes /0	Yes /0	No /1	Yes /0
Pfizer rule	No	Yes	No	Yes	Yes	Yes	Yes	Yes	Yes	No	No
Golden triangle	Yes	Yes	Yes	Yes	Yes	Yes	Yes	Yes	Yes	Yes	Yes
Pains	0	0	0	0	0	0	0	0	0	0	0
Druglike ness score	-0.27	-0.38	0.03	-0.23	-0.63	0.02	-0.40	0.05	-0.37	0.45	0.36
hERG blockers	0.114 /●	0.210 /●	0.155 /●	0.026 /●	0.124 /●	0.113 /●	0.074 /●	0.046 /●	0.154 /●	0.173 /●	0.188 /●
H. hepatotoxicity	0.136 /●	0.124 /●	0.197 /●	0.097 /●	0.118 /●	0.157 /●	0.142 /●	0.112 /●	0.146 /●	0.134 /●	0.216 /●
AMES toxicity	0.904 /●	0.979 /●	0.887 /●	0.845 /●	0.952 /●	0.762 /●	0.846 /●	0.826 /●	0.960 /●	0.879 /●	0.880 /●
Skin sensitisation	0.210 /●	0.604 /●	0.116 /●	0.278 /●	0.413 /●	0.180 /●	0.119 /●	0.255 /●	0.428 /●	0.157 /●	0.121 /●
Eye corrosion	0.003 /●	0.003 /●	0.003 /●	0.003 /●	0.003 /●	0.003 /●	0.003 /●	0.003 /●	0.003 /●	0.003 /●	0.003 /●
Caco-2	-4.915 /●	-4.808 /●	-4.859 /●	-4.929 /●	-4.849 /●	-4.928 /●	-4.943 /●	-4.932 /●	-4.850 /●	-4.903 /●	-4.839 /●
MDCK score	$2.4X10^{-5}$/●	$4.0X10^{-5}$/●	$2.2X10^{-5}$/●	$2.4X10^{-5}$/●	$5.4X10^{-5}$/●	$2.2X10^{-5}$/●	$2.2X10^{-5}$/●	$2.1X10^{-5}$/●	$3.8X10^{-6}$/●	$1.7X10^{-5}$/●	$2.2X10^{-5}$/●
Pgp-inhibitor	0.883 /●	0.197 /●	0.786 /●	0.103 /●	0.138 /●	0.072 /●	0.402 /●	0.053 /●	0.129 /●	0.586 /●	0.60 /●
HIA	0.004 /●	0.004 /●	0.005 /●	0.004 /●	0.004 /●	0.006 /●	0.005 /●	0.005 /●	0.005 /●	0.005 /●	0.005 /●
PPB (%)	99.55 /●	98.77 /●	99.59 /●	99.71 /●	98.98 /●	97.10 /●	96.97 /●	98.21 /●	97.09 /●	96.39 /●	97.46 /●
BBB	0.116 /●	0.129 /●	0.109 /●	0.104 /●	0.130 /●	0.085 /●	0.126 /●	0.086 /●	0.128 /●	0.069 /●	0.120 /●
CYP1A2 inhibitor	No /0.567	Yes /0.561	No /0.674	No /0.771	No /0.623	No /0.657	No /0.627	No /0.829	No /0.682	No /0.792	Yes /0.749
CYP2C19 inhibitor	Yes /0.899	Yes /0.856	Yes /0.922	Yes /0.958	Yes /0.927	Yes /0.928	Yes /0.958	Yes /0.965	Yes /0.949	Yes /0.945	Yes /0.938
CYP2C9 inhibitor	Yes /0.953	Yes /0.945	Yes /0.949	Yes /0.953	Yes /0.958	Yes /0.923	Yes /0.959	Yes /0.956	Yes /0.960	Yes /0.961	Yes /0.954
CYP2D6 inhibitor	No /0.314	Yes /0.229	No /0.446	No /0.665	No /0.487	No /0.850	No /0.482	No /0.640	No /0.463	No /0.508	No /0.416
CYP3A4 inhibitor	No /0.882	Yes /0.849	No /0.856	No /0.918	Yes /0.941	Yes /0.897	Yes /0.952	Yes /0.928	Yes /0.948	Yes /0.894	Yes /0.880
Sy. accessibility	2.870	2.969	2.885	2.985	3.013	2.981	2.903	2.961	2.994	2.861	2.865

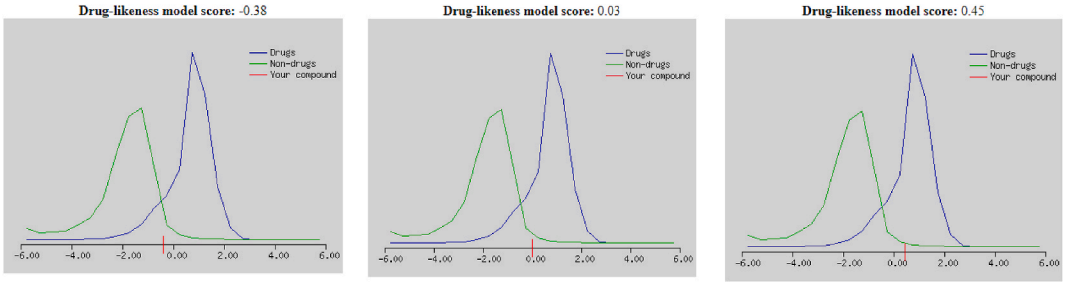

Fig. 6. Druglike ness modelscores of final triazoles **4b**, **4c**, and **4j**.

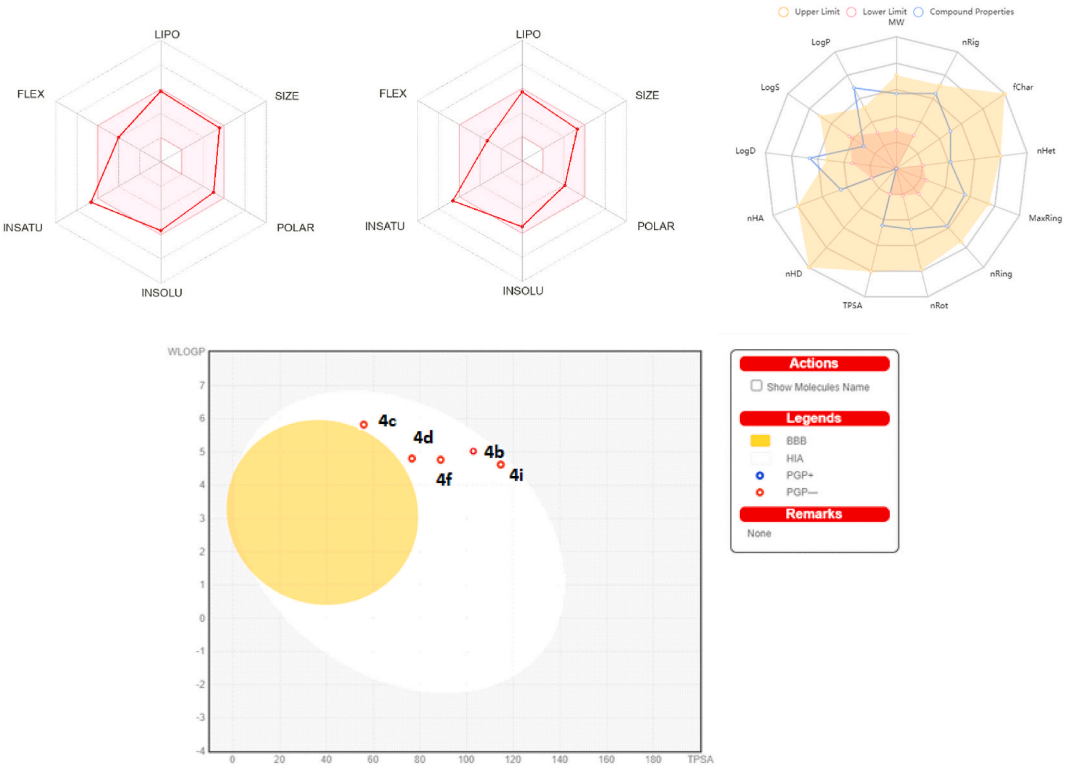

Fig. 7. Bioavailability radar and the BOILED-Egg model of synthesised molecules **4b**, **4c**, **4d**, **4f**, and **4i**.

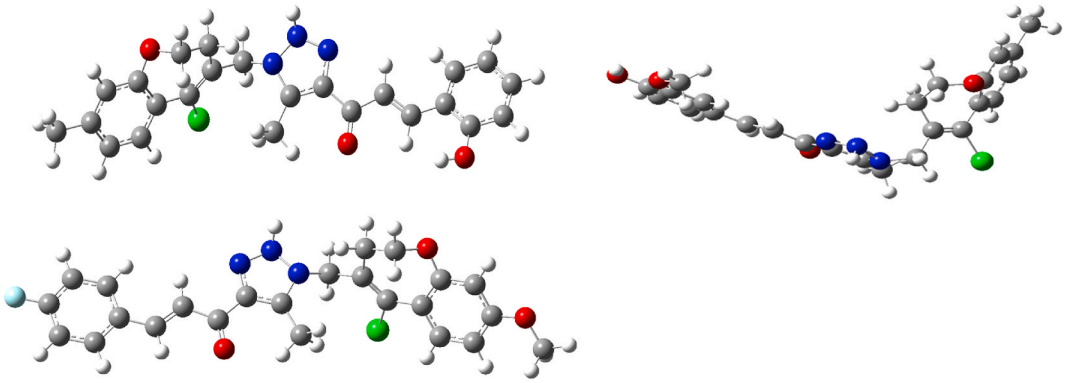

Fig. 8. Molecules **4d**, **4f** and **4k** are optimized at B3LYP/6-31g (d,p) level of theory in the gas phase.

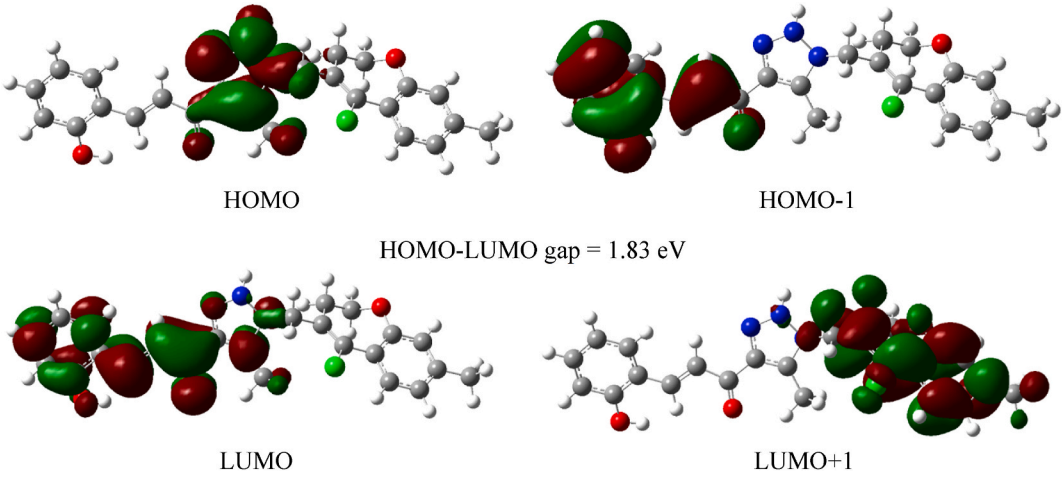

Fig. 9. The frontier molecular orbital (FMO) single point energy calculation carried out at B3LYP/6-31g (d,p)//B3LYP/6-31g (d,p) level of theory in the gas phase (**4d**).

LUMO band gap shows the potential of the molecule to act as a Inhibitor.

5. Experimental procedure

5.1. Materials and methods

Without undergoing additional purification, all of the chemicals were utilized directly from Sigma-Aldrich Chemicals (Dr. Reddy's laboratory, Hyderabad). The nitrogen atmosphere was used to conduct the moisture-sensitive processes. On aluminium foil that had been pre-coated with silica gel 60 F254 (Sigma–Aldrich, Bangalore), TLC analysis was performed. Melting points are uncorrected and were measured using a Thomas micro hot stage device. KBr solid discs + were used to determine the infrared spectra using a Shimadzu model 470 spectrophotometer. Using $CDCl_3$ and DMSO-d_6 as NMR solvents, ^{1}H NMR/^{13}C NMR spectra were acquired using a Jeol Eclipse 400, 100 MHz spectrometer. A JEOL JMS-600H apparatus was utilized to record mass spectra through the use of an electro spray ionization (ESI) detector. Using an Elementar Vario Micro Cube analyzer, elemental analysis was carried out, and all compound results were within ±0.4% of the expected values.

*5.2. General procedure for the synthesis of substituted 4-(azidomethyl)-5-chloro-2,3-dihydrobenzo [b]oxepine **1***

5.2.1. Preparation of 5-chloro-2,3-dihydrobenzo [b]oxepin-4-yl)methanol

A solution of 5-chloro-2,3-dihydrobenzo [*b*]oxepine-4-carbaldehyde (0.011 mol, 2.5 g) in dry ethanol (25 mL) was agitated at 0–5 °C while sodium borohydride (0.005 mol, 0.22 g) was slowly added. After the addition, the stirring was kept up for another 2 h at room temperature and TLC kept track of the reaction. The reaction was once more chilled to 0–5 °C once it was finished. It was extracted with ethyl acetate (2 × 50 mL) after being acidified using 1 N HCl. In order to separate the required alcohol, the mixed organic layers were concentrated under decreased pressure after being washed with brine and dried on anhydrous sodium sulphate. Without any purification, the raw alcohol was used for the following step.

5.2.2. Preparation of 5-chloro-4-(chloromethyl)-2,3-dihydrobenzo [b]oxepine

A magnetically agitated, ice-cold solution containing (5-chloro-2,3-dihydrobenzo [*b*]oxepin-4-yl) methanol (0.009 mol, 2 g), and pyridine (0.007 mol, 0.5 g), in dry benzene (10 mL), was added slowly after freshly distilled thionyl chloride (0.011 mol, 1.34 g) was added. The resulting mixture was stirred for 30 min at rt and then for 3 h at 80 °C. After the reaction was finished, the benzene was taken out to get the required chloro compound, which was used right away for the next step.

5.2.3. Preparation of 4-(azidomethyl)-5-chloro-2,3-dihydrobenzo [b]oxepine

Potassium iodide was added to the 5-chloro-4-(chloromethyl)-2,3-dihydrobenzo [*b*]oxepine (0.008 mol, 2 g) after it had been dissolved in dry acetone (20 mL) and magnetically agitated for an hour at room temperature. After that, aqueous sodium azide solution (0.010 mol, 0.67 g) was added to the reaction vessel, and TLC was used to track the reaction's development. When the reaction was complete, the mixture was placed to crushed ice, and ethyl acetate (2 × 50 mL) was used to extract it. Finally, azide was purified using column chromatography with an eluent ratio of 9:1 in petroleum ether to ethyl acetate.

5.3. Synthesis of 1-(1-((5-chloro-8-methyl-2,3-dihydrobenzo [b]oxepin-4-yl)methyl)-5-methyl-1H −1,2,3-triazol-4-yl)ethan-1-one **2**

In a 30 mL round bottom flask containing acetylacetone (0.024 mol, 2.40 g) and triethylamine (0.048 mol, 4.86 g) in dimethylformamide (30 mL), was added 4-(azidomethyl)-5-chloro-8-methyl-2,3-dihydrobenzo [*b*]oxepine **1** (0.012 mol, 3 g) portion wise at room temperature for overnight. It was finished and extracted with ethyl acetate before being washed with brine and water. To produce the crude product, the mixed organic layer was dried over sodium sulphate and allowed to evaporate. It was then possible to obtain 1-(1-((5-chloro-8-methyl-2,3-dihydrobenzo [b] oxepin-4-yl)methyl)-5-methyl-1H-1,2,3-triazol-4-yl)ethan-1-one **2** (91% yield over two steps) as a yellow solid by purifying the crude material using silica gel column chromatography (hexane/ethyl acetate 9:1).

5.4. Synthesis of chalcones bearing a 1,2,3-triazole unit

Following a previous procedure, the chalcone−triazole derivatives were synthesised. Triazole compound **2** (0.0084 mol, 2.8 g) and related aldehydes **3a−k** (0.0101 mol, 1.07 g) were combined with ethanol (28 mL) and agitated before being cooled in ice bath. Drop-by-drop additions of a sodium hydroxide ethanolic solution (0.152 mol, 6.08 g) were made while the mixture was continuously stirred for 10 min. After being brought to ambient temperature, the reaction was stirred over night. 200 mL of ice−cold water were used to dilute it, and after that, HCl solution was used to neutralise it. Pure (*E*)-chalcones **4a−k** carrying a 1,2,3−triazole scaffold were obtained from the produced solids after it had been filtered, washed excessively with ice−cold water, and dried. *General experimental details of spectral characterization, biological activity evaluation, computational docking studies and copies of ^{1}H NMR, ^{13}C NMR, IR and mass spectrums are included in supporting information.

6. Conclusion

All things considered, unique derivatives of benzooxapine−based triazolyl chalcones (**4a–k**) have been synthesised and shown by physical and spectral analysis, based on a new technique called “one drug-multiple targets” for finding novel treatments. *In vitro* biological activities, including antibacterial activity against Gram-(+ve) and Gram-(−ve) microorganisms, antifungal activity against fungal strains, and anti-tubercular activity against the H_{37}Rv strain of all 1,2,3-triazoles, were evaluated as part of the expanded investigation. The *in vitro* biological studies revealed that compounds **4c**, **4d**, **4f**, **4i**, and **4k** possessed multiple–active and exhibited potency as an antibacterial, antifungal, anti−tubercular activities among the other derivatives. Furthermore, the *in silico* study of most active chalcones **4d**, **4f**, and **4k** were performed against human Cytochrome P450 14 alpha-sterol demethylase (CYP51) from *M. tuberculosis* (PDB: 1EA1) and these compounds showed more stable docking energies confirming their plausible mode of action. Furthermore, according to the drug-likeness prediction, all of the prepared triazole–based chalcones (**4a–k**) met the requirements for drug-likeness, and as such, these derivatives–particularly the three that have drug-likeness scores of 0.03, 0.02, and 0.05, respectively and are recognized as novel drug candidates. Lastly, using SwissADME and ADMETlab2.0 platforms, the *in silico* ADMET properties data of the final 1,2,3-triazoles (**4a–k**) were further assessed for their ADMET and physicochemical characteristics. Therefore, benzooxapine-chalcone’s strong antibacterial activity and antitubercular characteristics connected to 1,2,3-triazole compounds can be leveraged to further modify and build new antimicrobial medicines.

Availability of data and materials

General experimental details of biological activity evaluation, computational docking studies and copies of ^{1}H NMR, ^{13}C NMR, Mass and IR spectrums are included in supporting information. The data that support the findings of this study are available in the supplementary material of this article.

CRediT authorship contribution statement

Sudhakar Reddy Baddam: Writing – original draft. **Mahesh Kumar Avula:** Resources. **Raghunadh Akula:** Validation, Data curation. **Venkateswara Rao Battula:** Formal analysis. **Sudhakar Kalagara:** Methodology, Formal analysis, Data curation. **Ravinder Buchikonda:** Visualization, Methodology. **Srinivas Ganta:** Project administration, Investigation. **Srinivasadesikan Venkatesan:** Visualization. **Tejeswara Rao Allaka:** Writing – review & editing, Writing – original draft, Software, Conceptualization.

Declaration of competing interest

The authors declare that they have no known competing financial interests or personal relationships that could have appeared to influence the work reported in this paper

Acknowledgements

The authors are thankful to Dr. Reddy’s Laboratories Pvt Ltd., for providing required facilities to completion of the research work. We also extend our gratitude towards JNTUH University for providing biological activities and molecular modelling techniques. VS also thankful to Center of Computational Facilities, VFSTR for the computational time.

Appendix A. Supplementary data

Supplementary data to this article can be found online at https://doi.org/10.1016/j.heliyon.2024.e27773.

References

[1] World Health Organization. https://www.who.int/news-room/fact-sheets/detail/tuberculosis, 2021 accessed on 6th September, 2022.
[2] Global Tuberculosis Report 2020, World Health Organization, Geneva, 2020.
[3] A. Chauhan, M. Kumar, A. Kumar, K. Kanchan, Life Sci. 274 (2021) 119301, https://doi.org/10.1016/j.lfs.2021.119301.
[4] A. Ginsberg, Drugs 70 (2010) 2201–2214, https://doi.org/10.2165/11538170-000000000-00000.
[5] S. Cole, R. Brosch, J. Parkhill, Nature 393 (1998) 537–544, https://doi.org/10.1038/31159.
[6] K. McLean, P. Carroll, D. Lewis, J. Biol. Chem. 283 (2008) 33406–33416, https://doi.org/10.1074/jbcM802115200.
[7] K.S. Parikh, D.S. Joshi, Med. Chem. Res. 22 (2013) 3688–3697, https://doi.org/10.1007/s00044-012-0369-3.
[8] R. Hasan, M. Acharjee, R. Noor, Tzu Chi Med. J. 28 (2016) 49–53, https://doi.org/10.1016/j.tcmj.2016.03.0021.
[9] N.T. Shivani, G.D. Amar, U.R. Bhavisha, N.P. Paresh, Chem. Phys. Lett. 817 (2023) 140426, https://doi.org/10.1016/j.cplett.2023.140426.
[10] S. Tandel, N.C. Patel, S. Kanvah, P.N. Patel, J. Mol. Struct. 1269 (2022) 133808, https://doi.org/10.1016/j.molstruc.2022.133808.
[11] S. Dadou, A. Altay, M. Koudad, B. Turkmenoglu, E. Yeniçeri, S. Çaglar, M. Allali, A. Oussaid, N. Benchat, K. Karrouchi, Med. Chem. Res. 31 (2022) 1369, https://doi.org/10.1007/s00044-022-02916-9.
[12] J. Cianci, J.B. Baell, B.L. Flynn, R.W. Gable, J.A. Mould, D. Paul, A.J. Harvey, Bioorg. Med. Chem. Lett. 18 (2008) 2055, https://doi.org/10.1016/j.bmcl.2008.01.099.
[13] S. Ahn, V.N.P. Truong, B. Kim, M. Yoo, Y. Lim, S.K. Cho, D. Koh, Appl. Biol. Chem. 65 (2022) 17, https://doi.org/10.1186/s13765-022-00686-x.
[14] G. Gogisetti, U. Kanna, V. Sharma, T. Rao Allaka, B. Rao Tadiboina, Chem. Biodivers. 19 (2022) e202200681, https://doi.org/10.1002/cbdv.202200681.
[15] S.G. Mansouri, H.Z. Boeini, K. Zomorodian, B. Khalvati, R.H. Pargali, A. Dehshahri, H.A. Rudbari, M. Sahihi, Z. Chavoshpour, Arab. J. Chem. 13 (2020) 1271, https://doi.org/10.1016/j.arabjc.2017.10.009.
[16] L.M. Linn, Y. Zhou, M.T. Flavin, L.M. Zhou, W. Nie, F.C. Chen, Bioorg. Med. Chem. 10 (2002) 2795, https://doi.org/10.1016/s0968-0896(02)00094-9.
[17] O.A. Oyedapo, C.O. Adewunmi, E.O. Iwalewa, V.O. Makanju, J. Biol. Sci. 8 (2008) 131–136, https://doi.org/10.3923/jbs.2008.131.136.
[18] A. Suyambulingam, S. Nair, K. Chellapandian, J. Mol. Struct. 1268 (2022) 133708, https://doi.org/10.1016/j.molstruc.2022.133708.
[19] A. Azam, F. Hayat, E. Mosely, S. Attar, R. Vanzyl, Eur. J. Med. Chem. 46 (2011) 1897, https://doi.org/10.1016/j.ejmech.2011.02.004.
[20] M. Satyanarayana, P. Tiwari, B.K. Tripathi, A.K. Srivastava, R. Pratap, Bioorg. Med. Chem. 12 (2004) 883, https://doi.org/10.1016/j.bmc.2003.12.026.
[21] L. Chen, W. Fu, L. Zheng, Z. Liu, G. Liang, J. Med. Chem. 61 (2018) 4290, https://doi.org/10.1021/acs.jmedchem.7b01310.
[22] K. Chand, A.N. Shirazi, P. Yadav, R.K. Tiwari, M. Kumari, K. Parang, S.K. Sharma, Can. J. Chem. 91 (2013) 741, https://doi.org/10.1139/cjc-2013-0053.
[23] F.F. Ahmed, A.A. Abd El-Hafeez, S.H. Abbas, D. Abdelhamid, M.A. Aziz, Eur. J. Med. Chem. 151 (2018) 705–722.
[24] I. Jantan, S.N.A. Bukhari, O.A. Adekoya, I. Sylte, Drug Des. Dev. Ther. 8 (2014) 1405–1418.
[25] C.I. Liu, G.Y. Liu, Y. Song, F. Yin, M.E. Hensler, W.Y. Jeng, V. Nizet, A.H. Wang, E. Oldfield, Science 319 (2008) 1391–1394.
[26] C.S. Takeuchi, B.G. Kim, C.M. Blazey, S. Ma, H.W.B. Johnson, N.K. Anand, A. Arcalas, T.G. Baik, C.A. Buhr, J. Cannoy, S. Epshteyn, A. Joshi, K. Lara, M.S. Lee, L. Wang, J.W. Leahy, J.M. Nuss, N. Aay, R. Aoyama, P. Foster, J. Lee, I. Lehoux, N. Munagala, A. Plonowski, S. Rajan, J. Woolfrey, K. Yamaguchi, P. Lamb, N. Miller, J. Med. Chem. 56 (2013) 2218–2234.
[27] B. Capuano, I.T. Crosby, F.M. McRobb, D.A. Taylor, A. Vom, W.W. Blessing, Prog. Neuro-Psychopharmacol. Biol. Psychiatry 34 (2010) 136–142.
[28] A. Afanasenko, K. Barta, iScience 24 (2021) 102211.
[29] M.R. Aouad, M.A. Almehmadi, N. Rezki, F.F. Al-blewi, M. Messali, I. Ali, J. Mol. Struct. 1188 (2019) 153–164.
[30] A. Rani, G. Singh, A. Singh, U. Maqbool, G. Kaur, J. Singh, RSC Adv. 10 (2020) 5610–5635.
[31] J.F. Liegeois, M. Deville, S. Dilly, C. Lamy, F. Mangin, M. Resimont, F.I. Tarazi, J. Med. Chem. 55 (2012) 1572–1582.
[32] S.S. Braga, Eur. J. Med. Chem. 183 (2019) 111660.
[33] X.M. Chu, C. Wang, W. Liu, L.L. Liang, K.K. Gong, C.Y. Zhao, K.L. Sun, Eur. J. Med. Chem. 161 (2019) 101.
[34] M.J. Genin, D.A. Allwine, D.J. Anderson, M.R. Barbachyn, D.E. Emmert, S.A. Garmon, D.R. Graber, K.C. Grega, J.B. Hester, D.K. Hutchinson, J. Morris, R. J. Reischer, C.W. Ford, G.E. Zurenco, J.C. Hamel, R.D. Schaadt, D. Stapertand, B.H. Yagi, J. Med. Chem. 43 (2000) 953–970.
[35] G. Gopalarao, T.R. Allaka, U.R. Kanna, B. Sravanthi, R.K. Ganta, V. Sharma, B.T. Rao, Russ. J. Bioorg. Chem. 49 (2023) 634, https://doi.org/10.1134/S1068162023030111.
[36] Şahin İrfan, Mustafa Çeşme, Neslihan Yüce, Ferhan Tümer, J. Biomol. Struct. Dyn. 41 (2023) 1988–2001, https://doi.org/10.1080/07391102.2022.2025905.
[37] Şahin İrfan, Mustafa Çeşme, Fatma Betül Özgeri, Ferhan Tümer, Chem. Biol. Interact. 370 (2023) 110312, https://doi.org/10.1016/j.cbi.2022.110312.
[38] R.M. Kumbhare, U.B. Kosurkar, M.J. Ramaiah, T.L. Dadmal, S.N.C.V.L. Pushpavalli, M. PalBhadra, Bioorg. Med. Chem. Lett. 22 (2012) 5424–5427.
[39] C. Hager, R. Miethchen, H. Reinke, J. Fluor. Chem. 104 (2000) 135–142.
[40] A.K. Jordao, P.P. Afonso, V.F. Ferreira, M.C. de Souza, M.C. Almeida, C.O. Beltrame, D.P. Paiva, S.M. Wardell, J.L. Wardell, E.R. Tiekink, C.R. Damaso, A. C. Cunha, Eur. J. Med. Chem. 44 (2009) 3777–3783.
[41] P. Singh, R. Raj, V. Kumar, M.P. Mahajan, P.M.S. Bedi, T. Kaur, A.K. Saxena, Eur. J. Med. Chem. 47 (2012) 594–600.
[42] I. Mohammed, I.R. Kummetha, G. Singh, N. Sharova, G. Lichinchi, J. Dang, M. Stevenson, T.M. Rana, J. Med. Chem. 59 (2016) 7677–7682.
[43] X.-M. Chu, C. Wang, W.-L. Wang, L.-L. Liang, W. Liu, K.-K. Gong, K.-L. Sun, Eur. J. Med. Chem. 166 (2019) 206–223.
[44] B.J. McConkey, V. Sobolev, M. Edelman, Curr. Sci. 83 (2002) 845–855.
[45] G. Venkateswara Rao, B. Hari Babu, A. Tejeswara Rao, V. Pandu Ranga Rao, B. Sravanthi, G. Mutyalanaidu, P. Santhosh Reddy, Chem. Biodivers. 20 (2023) e202201259, https://doi.org/10.1002/cbdv.202201259.
[46] G.I. Lepesheva, M.R. Biophys, Acta 1814 (2011) 88–93.
[47] H.R. Superko, K.M. Momary, Y. Li, Med. Clin. 96 (2012) 123–139.
[48] V. Satheeshvarma, B. Rajashaker, J. Nishant, J. Sridhara, N. Lingaiah, Bioorg. Med. Chem. Lett. 30 (2020) 127304.
[49] H.F. Ashour, L.A. Abou-zeid, M.A.-A. El-Sayed, K.B. Selim, Eur. J. Med. Chem. 189 (2020) 112062.
[50] B.H.M. Mruthyunjaya Swamy, S.M. Basavarajaiah, Indian J. Chem. B 48B (9) (2009) 1274–1282.
[51] S.K. Gandham, A.A. Kudale, T.R. Allaka, A. Jha, ChemistrySelect 7 (2022) e202200683, https://doi.org/10.1002/slct.202200683.
[52] N.M. O'Boyle, M. Banck, C.A. James, J. Cheminf. 3 (2011) 33, https://doi.org/10.1186/1758-2946-3-33.
[53] L.M. Podust, T.L. Poulos, M.R. Waterman, Proc. Natl. Acad. Sci. U. S. A. 98 (2001) 3068, https://doi.org/10.1073/pnas.061562898.
[54] T.R. Allaka, B. Kummari, N. Polkam, N. Kuntala, K. Chepuri, J.S. Anireddy, Mol. Divers. 26 (2022) 1581, https://doi.org/10.1007/s11030-021-10287-3.
[55] G.M. Morris, R. Huey, W. Lindstrom, M.F. Sanner, R.K. Belew, D.S. Goodsell, A.J. Olson, J. Compt. Chem. 16 (2009) 2785, https://doi.org/10.1002/jcc.21256.
[56] S.A. Hassan, N.M. Morsy, W.M. Aboulthana, A. Ragab, RSC Adv. 13 (2023) 9281, https://doi.org/10.1039/d3ra00297g.
[57] E.S.A.E.H. Khattab, A. Ragab, M.A. Abol-Ftouh, A.A. Elhenawy, J. Biomol. Struct. Dyn. 40 (2022) 1–19.
[58] A.S. Hassan, N.M. Morsy, W.M. Aboulthana, A. Ragab. Drug. Dev. Res. 84 (2023) 3–24, https://doi.org/10.1002/ddr.22008.

[59] D. Ananda Kumar, A. Tejeswara Rao, K. Yugandhar, N. Sunil Kumar, P. Pradeep, K. Chandrasekhar, PVVN. Kishore. Cur. Org. Synth. 20 (2023) 576, https://doi.org/10.2174/1570179419666220822125724.
[60] G. Xiong, Z. Wu, J. Yi, L. Fu, Z. Yang, C. Hsieh, M. Yin, X. Zeng, C. Wu, A. Lu, X. Chen, T. Hou, D. Cao, Nucleic Acids Res. 49 (2021), https://doi.org/10.1093/nar/gkab255. W5.
[61] J. Hakkola, J. Hukkanen, M. Turpeinen, O. Pelkonen, Arch. Toxicol. 94 (2020) 3671, https://doi.org/10.1007/s00204-020-02936-7.